White Matter Damage and Systemic Inflammation in Obstructive Sleep Apnea

Hsiu-Ling Chen, MD[1,2]; Cheng-Hsien Lu, MD, PhD[3,4]; Hsin-Ching Lin, MD[5,6]; Pei-Chin Chen, MSc[1]; Kun-Hsien Chou, PhD[7]; Wei-Ming Lin, MD[8]; Nai-Wen Tsai, MD, PhD[3]; Yu-Jih Su, MD[4,9]; Michael Friedman, MD[10,11]; Ching-Po Lin, PhD[2,12,*]; Wei-Che Lin, MD, PhD[1,*]

*[1]Department of Diagnostic Radiology, Kaohsiung Chang Gung Memorial Hospital, and Chang Gung University College of Medicine, Kaohsiung, Taiwan; [2]Department of Biomedical Imaging and Radiological Sciences, National Yang-Ming University, Taipei, Taiwan; [3]Department of Neurology, Kaohsiung Chang Gung Memorial Hospital, and Chang Gung University College of Medicine, Kaohsiung, Taiwan; [4]Department of Biological Science, National Sun Yat-Sen University, Kaohsiung, Taiwan; [5]Department of Otolaryngology, Kaohsiung Chang Gung Memorial Hospital, and Chang Gung University College of Medicine, Kaohsiung, Taiwan; [6]Sleep Center, Kaohsiung Chang Gung Memorial Hospital and Chang Gung University College of Medicine, Kaohsiung, Taiwan; [7]Brain Research Center, National Yang-Ming University, Taipei, Taiwan; [8]Department of Diagnostic Radiology, Chiayi Chang Gung Memorial Hospital and Chang Gung University College of Medicine, Chiayi, Taiwan; [9]Department of Internal Medicine, Kaohsiung Chang Gung Memorial Hospital, and Chang Gung University College of Medicine, Kaohsiung, Taiwan; [10]Department of Otolaryngology-Head and Neck Surgery, Division of Sleep Surgery, Rush University Medical Center, Chicago, IL; [11]Department of Otolaryngology, Advanced Center for Specialty Care, Advocate Illinois Masonic Medical Center, Chicago, IL; [12]Institute of Neuroscience, National Yang-Ming University, Taipei, Taiwan; *co-last authors*

Study Objectives: To evaluate white matter integrity in patients with obstructive sleep apnea (OSA) using diffusion tensor imaging (DTI) and to assess its relationship with systemic inflammation.

Design: Cross-sectional study.

Setting: One tertiary medical center research institute.

Patients or Participants: Twenty patients with severe OSA (apnea-hypopnea index [AHI] > 30, 18 men and 2 women) and 14 healthy volunteers (AHI < 5, 11 men and 3 women).

Interventions: N/A.

Measurements and Results: Patients with severe OSA and healthy volunteers underwent polysomnography to determine the severity of sleep apnea, and DTI scanning to determine fiber integrity. Early or late phase changes in leukocyte apoptosis and its subsets were determined by flow cytometry. DTI-related indices (including fractional anisotropy [FA], axial diffusivity [AD], radial diffusivity [RD], and mean diffusivity [MD]) were derived from DTI. The FA maps were compared using voxel-based statistics to determine differences between the severe OSA and control groups. The differences in DTI indices, clinical severity, and leukocyte apoptosis were correlated after adjusting for age, sex, body mass index, and systolic blood pressure. Exploratory group-wise comparison between the two groups revealed that patients with OSA exhibited low FA accomplished by high RD in several brain locations, without any differences in AD and MD. The FA values were negatively correlated with clinical disease severity and leukocyte early apoptosis.

Conclusions: Obstructive sleep apnea impairs white matter integrity in vulnerable regions, and this impairment is associated with increased disease severity. The possible interactions between systemic inflammation and central nervous system microstructural damage may represent variant hypoxic patterns and their consequent processes in obstructive sleep apnea.

Keywords: diffusion tensor imaging, leukocyte apoptosis, magnetic resonance imaging, obstructive sleep apnea, oxidative stress

Citation: Chen HL, Lu CH, Lin HC, Chen PC, Chou KH, Lin WM, Tsai NW, Su YJ, Friedman M, Lin CP, Lin WC. White matter damage and systemic inflammation in obstructive sleep apnea. *SLEEP* 2015;38(3):361–370.

INTRODUCTION

Obstructive sleep apnea (OSA) is the most common type of breathing disorder in sleep. Recent evidence has shown that OSA is highly correlated with the development of cardiovascular and cerebrovascular diseases.[1,2] Oxidative stress and subsequent inflammation are uniquely triggered by apnea-related intermittent hypoxia.[3] Accumulated evidence has demonstrated that leukocyte-endothelial cell activation and adhesion induce inflammation and damage to the vasculature, increasing the risk of cardiovascular complications.[4] However, the role of inflammation markers in peripheral blood related to OSA has not been systematically investigated with critical insights.

Repetitive hypoxia/reoxygenation associated with transient cessation of breathing during apneas and hypopneas is considered the main culprit for the endothelial dysfunction in OSA. Several systemic inflammatory markers have been demonstrated to be involved during endothelial damage. Endothelial progenitor cells (EPCs) are released from the bone marrow to the peripheral blood and participate in endothelial cell repair and regeneration. Clinical studies have revealed that cardiovascular diseases are associated with dysfunction in EPCs, and that the number of circulating EPCs correlates positively with clinical outcome.[5] The interface between vascular endothelium and host inflammatory response can also be associated with the activation of resident microglia, astrocytes, and peripheral blood leukocytes,[6] as well as with the expression

Submitted for publication March, 2014
Submitted in final revised form June, 2014
Accepted for publication July, 2014

Address correspondence to: Ching-Po Lin, PhD, Department of Biomedical Imaging and Radiological Sciences, Institute of Neuroscience, National Yang-Ming University, 155 Li-Nong Street, Section 2, Peitou, Taipei, Taiwan; Tel: 886-2-28267338; Fax: 886-2-28262285; Email: cplin@ym.edu.tw and Wei-Che Lin, MD, PhD, Department of Diagnostic Radiology, Kaohsiung Chang Gung Memorial Hospital, Chang Gung University College of Medicine, 123 Ta-Pei Road, Niao-Sung, Kaohsiung 83305, Taiwan; Tel: +886-7-731-7123 ext 3027; Fax: +886-7-731-7123 ext 2523; Email: u64lin@yahoo.com.tw

of inflammatory cytokines and adhesion molecules.[7] Furthermore, injured endothelium promotes inflammation along the vessel wall that is mediated by soluble leukocyte-selectin (sL-selectin), soluble endothelial-selectin (sE-selectin), and soluble platelet-selectin (sP-selectin), all of which bind to circulating leukocytes.[8] Subsequent adhesion to endothelial ligands for soluble intercellular (sICAM-1) and soluble vascular cell adhesion molecules (sVCAM-1) allows leukocyte transmigration into the damaged tissues. However, the role of these inflammatory markers in the pathogenesis of OSA remains unknown.

In addition, oxidative stress has been demonstrated to have a prominent role in the pathogenesis of demyelination and tissue injury in multiple sclerosis.[9] Direct oxidative damage occurs across many brain regions, and axons may be damaged by stress-related compounds associated with high baseline sympathetic tone or sleep deprivation.[10] Previous studies in a rat model have shown that chronic intermittent hypoxia increases brain cortical neuronal cell death.[11] The diagnosed neurologic disease reflects the extreme clinical presentation of the pathologic processes. One method for evaluating the early preclinical changes of OSA is magnetic resonance imaging (MRI).

Diffusion tensor imaging (DTI), an MRI sequence, is potentially more sensitive for detecting intracranial microstructural change than conventional MRI. Among various quantitative parameters such as apparent diffusion coefficient (ADC) and eigenvalues derived from DTI, fractional anisotropy (FA) is recognized as the most useful for evaluating the integrity of white matter (WM) fibers. Changes in WM integrity in OSA has been reported using DTI, including a global brain decrease in mean diffusivity values and that certain regional sites are especially affected by decreased FA values.[12,13] However, the correlation, if any, between WM alterations and disease severity in OSA has not been well evaluated.

The current study targeted WM integrity and aimed to explore the pathophysiology of OSA. First, the levels of systemic inflammatory markers and the effects of sleep apnea on the WM were investigated in patients with OSA and healthy controls. Second, the differences in WM as determined by the direct comparison of the groups were associated with disease severity in the patients with OSA. Third, the relationships between WM integrity alteration and the effects of systemic inflammation were also investigated. It is hypothesized that the increased circulation of inflammatory markers in patients with OSA correlates with the severity of sleep disturbance and the reduction in WM integrity.

PATIENTS AND METHODS

Patients

This prospective study targeted patients with severe OSA (apnea-hypopnea index [AHI] ≥ 30). Twenty patients with severe OSA (18 men and 2 women; mean age, 38.60 ± 9.85 years; body mass index [BMI], 27.13 ± 3.35 kg/m^2; AHI, 58.89 ± 14.51 events/h), and 14 healthy volunteers (11 men and 3 women; mean age, 38.21 ± 9.89 years; BMI, 23.84 ± 2.66 kg/m^2, AHI, 2.86 ± 1.30 events/h) were recruited.

All patients with OSA and control subjects were enrolled through the sleep center with a chief complaint of snoring. The severity of sleep disordered breathing was classified according to the number of apneas and hypopneas during sleep, reported as the AHI. All participants underwent an overnight polysomnography (PSG) study at the Kaohsiung Chang Gung Memorial Hospital, and were scored and classified into patient and control groups according to standard diagnostic criteria.[14] All those in the patient group recently received a diagnosis and had not yet been treated for OSA. None had a history of major mental disorder, brain injury or illness, diabetes mellitus, cerebrovascular disease, major cardiovascular disorder (e.g., stroke, heart failure, myocardial infarction), or any central/peripheral disorders known to affect autonomic nervous systems. An experienced neuroradiologist blinded to the participants' status visually checked all of the MRI scans to ensure that the participants were free from significant brain injury. None of the participants in the study was excluded.

The Chang Gung Memorial Hospital Ethics Committee approved the study and all of the participants provided written informed consent.

Assessment of Obstructive Sleep Apnea/Hypopnea by PSG

The overnight PSG data were assessed according to a previous report.[15] All-night attended and comprehensive diagnostic sleep studies were performed at the hospital's sleep center, in a temperature-controlled and sound-attenuated room. Electroencephalography (EEG), submental electromyography, and electro-oculography were recorded with surface electrodes using standard techniques. Nasal and oral airflows were recorded by thermistors, whereas oxygen saturation was measured by pulse oximetry. By definition, obstructive apnea was a cessation of airflow for at least 10 sec with effort to breathe during the cessation. Obstructive hypopnea was defined as an abnormal respiratory event with at least a 30% reduction in thoracoabdominal movement or airflow when compared to baseline, lasting at least 10 sec, with < 4% oxygen desaturation.[16] The AHI was calculated per hour of EEG sleep. Central respiratory events were excluded from severity classification.

The OSA severity was classified as normal for an AHI between 0–5, mild for an AHI of 5–15, moderate for an AHI > 15 and < 30, and severe for an AHI > 30.[14] For comparison, participants categorized in the control group all had an AHI score of < 5. The oxygen desaturation index was defined by the number of times per hour of sleep that the blood's oxygen level dropped from the baseline. The snoring index was defined as: (total time with snoring > 90 dB/estimated total sleep time) × 100. Records were scored for sleep stages according to the criteria of Rechtshaffen and Kales.[17] All PSG tests were scored and read by a board-certified physician blinded to the study.

Blood Sampling and Laboratory Investigations

Blood samples were collected from the patients with OSA and controls by venipuncture of forearm veins.

Assessment of Leukocyte Apoptosis

The condition of leukocyte apoptosis was assessed with APO 2.7-PE to identify early apoptosis and late apoptosis. Positive expression of APO 2.7-PE indicated the presence of apoptotic cells. Further analysis of early and late apoptosis was conducted by annexin V-FITC and 7-aminoactinomycin D (7-AAD). The presence of late apoptotic cells meant that the

cell membrane integrity was disrupted. The presence of early apoptotic cells indicated that the apoptotic change was early and still reversible.

A whole blood sample (100 μL) was stained with 10 μL CD45-phycoerythrin (PE)-Cy5 (clone J33; Immunotech, Marseille, France) for 15 min at room temperature while protected from light. The CD45-PE-Cy5 antibody reacted with the CD45 family of transmembrane glycoproteins expressed on the surface of all human leukocytes and was a panleukocyte marker. Cells were fixed with 5.5% formaldehyde and washed with phosphate buffered saline (PBS). Then 100 μL IntraPrep permeabilization reagent (Immunotech) was added to each sample and the cells were incubated for 5 min at room temperature without shaking. During this stage, the cells were brought into contact with APO 2.7-PE (clone 2.7A6A3; Immunotech) to determine intracellular antigens. The APO 2.7-PE antibody reacted with a 38 kDa mitochondrial membrane protein (7A6 antigen) that was detectable in nonpermeabilized cells during the late apoptotic state.[18] Mouse immunoglobulin G (IgG)-PE was used as a control for nonspecific staining. The leukocytes were then analyzed by flow cytometry.

Flow cytometry analysis was performed immediately after staining with an Epics XL flow cytometer (Beckman Coulter, USA) using EXPO32 ADC software. Leukocytes and their subtypes were identified by CD45-PE-Cy5-positive and side-scatter gating. A minimum of 5,000 events was collected for total leukocytes in every blood sample. Leukocyte subtypes were identified based on the intensity of CD45 expression. Results were expressed as a percentage of specific fluorescence-positive cells. Apoptotic cells were defined as those that were positive for APO 2.7. A database coordinator monitored all data collection and entry, both of which were checked for any inconsistencies.

Membrane phosphatidyl-serine was detected by annexin-V using a commercially available kit (Boehringer Mannheim, Indianapolis, IN, USA). PBS washed leukocytes were incubated with annexin V-FITC and 7-aminoactinomycin D (7-AAD) for 15 min on ice according to manufacturer guidelines. Immediately thereafter, samples were analyzed with an Epics XL flow cytometer. Fifteen thousand events were counted per sample. Low-fluorescence debris was gated out of the analysis. Leukocyte subtypes were identified according to their CD45 expression intensity. Annexin V-FITC staining was identified in FL-1, and 7-AAD staining was identified in FL-4. Cells were identified as early apoptotic cells if they were positive for marker annexin V-FITC but negative for 7-AAD. Cells were identified as late apoptotic cells if they were positive for annexin V-FITC and 7-AAD. Cells were identified as dead cells if they were negative for annexin V-FITC but positive for 7-AAD. Finally, cells were identified as viable cells if they were negative for both annexin V-FITC and 7-AAD.

Assessment of Circulating Endothelial Progenitor Cell Levels

EPCs derived from peripheral blood were identified by flow cytometry based on a previous report.[19] To determine the EPC surface markers of CD45/CD34, CD45/CD133, KDR/CD133, and KDR/CD34, mononuclear cells (10^6) were incubated for 30 min at 4°C in a dark room with monoclonal antibodies against kinase insert domain-conjugating receptor (KDR) (Miltenyi Biotec, Bergisch Gladbach, Germany), fluorescein isothiocyanate-conjugated CD34, CD133, and PE-conjugated CD45 (Backman Coulter, USA). The control ligand (IgG-fluorescein isothiocyanate conjugate) was used to detect any nonspecific association and to define a threshold for glycoprotein binding.

For analysis of KDR, the mononuclear cells were further incubated with PE conjugated antimouse antibody made in goats. After staining, the mononuclear cells were fixed in a 1% solution of paraformaldehyde. Quantitative two-color flow cytometric analysis was performed using an Epics XL flow cytometer (Beckman Coulter). Each analysis included 10,000 cells per sample. The assays for the EPCs in each sample were performed in duplicate, with mean level reported.

Assessment of Serum Adhesion Molecules

Serum sICAM-1, sVCAM-1, sE-selectin, sL-selectin, and sP-selectin levels were assessed using commercially available enzyme-linked immunosorbent assays (R&D Systems, Minneapolis, MN, USA) as previously described.[20] In these assays, standards, controls, and unknown samples were incubated in microtitration wells coated with marked (i.e., anti-ICAM-1, VCAM-1, P-selectin, E-selectin, and L-selectin) antibodies. After incubation and washing, the wells were treated with another antiantigen detection antibody labeled with enzyme horseradish peroxidase.

After a second incubation and washing step, the wells were incubated with substrate tetramethylbenzidine. An acidic stopping solution was then added and the degree of enzymatic turnover of the substrate was determined by a dual-wavelength absorbance measurement at 450 and 620 nm. Absorbance was directly proportional to the concentration of antigens present. A set of standard antigen was used to plot a standard curve of absorbance versus antigen concentration from which the antigen concentrations of the unknowns were calculated.

MRI Data Acquisition

Data Acquisition

The MRI scan was performed using a 3.0 Tesla whole-body GE Signa MRI system (General Electric Healthcare, Milwaukee, WI, USA) equipped with an eight-channel head coil. DTI was conducted along the anterior-posterior commissure line (AC-PC line) in the axial plane using single shot spin-echo echoplanar imaging (EPI) sequence (repetition time/echo time [TR/TE] = 15,800/77 ms, number of excitation [NEX] = 3, matrix size = 256 × 256, field of view [FOV] = 25.6 cm, voxel size = 1 × 1 × 2.5 mm^3, 55 slices without gaping). The diffusion images gradient encoding schemes included 13 noncollinear directions with b-value 1000 s/mm^2 and a nondiffusion weighted image volume (b-value 0 s/mm^2).

The T1-weighted image was also acquired along the AC-PC line and used three-dimensional fluid-attenuated inversion-recovery fast spoiled gradient recalled echo sequence (3D IR-FSPGR, TR/TE/inversion time = 9.5/3.9/450 ms, flip angle = 20°, FOV = 25.6cm, matrix size = 512 × 512, voxel size = 0.47 × 0.47 × 1.3 mm^3, 110 slices without gaping). An axial T2-weighted image was acquired using fast spin-echo sequence (TR/TE = 4,200/102 ms, NEX = 2, matrix size = 320 × 256; FOV = 24 cm; echo train length = 18, slice thickness = 5

mm). The T1- and T2- weighted images were used to identify any brain abnormality. The total scanning time for this protocol was 20 min for each participant.

Data Preprocessing

The magnetic resonance images were preprocessed using the FSL v5.0.4 (Functional Magnetic Resonance Imaging of the Brain (FMRIB) Software Library, Oxford, UK; http://www.fmrib.ox.au.uk/fsl), including eddy current correction and brain tissue extraction.[21] Each diffusion-weighted image was registered to the nondiffusion weighted image by an affine registration approach that was supplied in FMRIB's Linear Image Registration Tool (FLIRT; part of FSL), which was used not only to minimize image distortion from eddy currents induced by fast-switching gradient coil, but also to reduce image distortion due to simple head motion. The images were then skull-stripped to remove nonbrain tissue and background noise using the Brain Extraction Tool (BET; part of FSL). A diffusion tensor model was fitted in each voxel using FMRIB's Diffusion Toolbox (FDT, part of FSL) for calculation of FA values, axial diffusivity (AD), λ1, radial diffusivity (RD), [(λ2+λ3)/2]), and mean diffusivity (MD), [(λ1+λ2+λ3)/3).

The Montreal Neurological Institute (MNI) space served as the standard template space for group comparison in this study. The FMRIB58_FA standard space image, a high-resolution average of 58 well-aligned good quality FA images in FSL, was used as the target image. Each subject's FA image was spatially normalized to the target image with a nonlinear registration using FMRIB's Non-Linear Image Registration Tool (FNIRT, part of FSL). The final voxel size of an image was resampled to 1 mm cubic resolution. All normalized FA images were smoothed with 8-mm Gaussian kernel.

Statistical Analysis

Analysis of Demographic Data Between Groups

The statistical analysis was performed using the Statistical Package for Social Sciences (SPSS) software package (version 17, SPSS Inc. Chicago, IL, USA). Age and sex were compared between the study groups by the independent *t* test and Pearson chi-square test. An analysis of covariance (ANCOVA) model with age and sex as covariates was used to determine differences in the BMI scores between the groups. ANCOVA with age, sex, and BMI as potential confounding variables was used to compare the groups in terms of AHI score, desaturation index, snoring index, average O_2 saturation, blood sugar, HbA1c, and systolic blood pressure (BP). ANCOVA with age, sex, BMI, and systolic BP as potential confounding variables was used to compare the group differences in laboratory data in terms of the percentage of leukocyte apoptosis, circulating endothelial progenitor cell level, and serum adhesion molecules. Statistical significance was set at $P < 0.05$.

Analysis of Group Comparison of FA Values

Statistical analyses were conducted using the SPM8 (Statistical Parametric Mapping; http://www.fil.ion.ucl.ac.uk/spm/; University College London, London, UK), which used the Matlab R2010a (Mathworks, Natick, MA, USA) for voxelwise group comparisons. Smoothed, normalized FA images were analyzed by SPM8 within the framework of a General Linear Model, whereas ANCOVA was performed with age and sex as covariates to investigate the FA differences between the OSA and control groups. The FA threshold of the mean WM was set at 0.2 to successfully exclude voxels, which consisted of gray matter or cerebrospinal fluid in most subjects. The statistical threshold was set at an uncorrected $P < 0.005$, with a cluster of > 100 contiguous voxels. The extended cluster size was arbitrary and was used to putatively detect significant differences between groups with a cluster size < 100 voxels, which might not represent reliable findings.[12]

The most probable fiber tracts and anatomic location of each significant cluster were determined using the FSL atlas tool (http://www.fmrib.ox.ac.uk/fsl/fslwiki/Atlases).

Analysis of Region of Interest

Analysis of region of interest (ROI) was made to determine the mean FA value of each significantly different area between the two groups based on whole brain voxelwise comparisons. The Marsbar toolbox (http://marsbar.sourceforge.net/download.html) was used to extract the ROI masks. The mean DTI-related indices (including FA, AD, RD, and MD) of these areas were compared between groups by multivariate analysis of covariance, with age, sex, BMI, and systolic BP as covariates. Significance was set at a Bonferroni corrected $P < 0.05$, accounting for multiple ROI comparisons.

Correlation Among Regional DTI-Related Indices, Clinical Severity, and Leukocyte Apoptosis

Partial correlation analysis adjusted for age, sex, BMI, and systolic BP was performed to correlate the clinical severity and leukocyte apoptosis with the regional DTI-related indices in the patient group. The threshold for statistical significance was set at $P < 0.05$ with Bonferroni correction for multiple comparisons.

RESULTS

Demographic Characteristics of the Participants

The demographic characteristics of the 20 severe OSA cases and 14 controls are listed in Table 1. There were no significant differences in age and sex between the two groups. However, patients with severe OSA had significantly increased BMI compared to controls. The severe OSA group also had significantly increased desaturation index, decreased average O_2 saturation during sleep, and increased snoring index compared to the control group.

Leukocyte Apoptosis between Groups

Leukocyte apoptosis levels in the two groups were determined by flow cytometry. The percentages of early apoptosis of total leukocytes and their subsets, including granulocytes, monocytes, and lymphocytes, were significantly higher in the OSA group than in the controls (Figure 1).

Changes in Circulating EPCs and Soluble ICAM Levels between Groups

There were no significantly different changes in the level of $CD133^+/CD34^+$ EPCs and $KDR^+/CD34^+$ EPCs between the two groups (Table 2). Patients with severe OSA also did not

Table 1—Demographic characteristics of patients with severe obstructive sleep apnea and control subjects.

	Severe OSA	Normal Control	P
Number	20	14	
Age	38.60 ± 9.85	38.21 ± 9.89	0.911
Sex (M:F)	18:2	11:3	0.354
BMI	27.13 ± 3.35	23.84 ± 2.66	0.008 [a]
AHI	58.89 ± 14.51	2.86 ± 1.30	< 0.001 [a]
Desaturation index	49.55 ± 19.46	0.94 ± 0.75	< 0.001 [a]
Average O_2 saturation	93.97 ± 2.38	97.19 ± 0.81	0.001 [a]
Snoring index	441.06 ± 144.60	231.16 ± 237.48	0.031 [a]
Sugar	92.65 ± 7.96	90.17 ± 6.15	0.866
HbA1c	5.85 ± 0.45	5.47 ± 1.49	0.086
Systolic BP (mmHg)	139.63 ± 11.81	124.68 ± 16.45	0.089

Age data were compared by independent *t* test. Sex data were compared by Pearson chi-square test. BMI data were compared by analysis of covariance (ANCOVA) after controlling for age and sex. AHI score, desaturation index, average O_2 saturation, snoring index, sugar, HbA1c, and systolic BP data were compared by ANCOVA after controlling for age, sex, and BMI. Data are presented as mean ± standard deviation. [a] P < 0.05. AHI, apnea-hypopnea index; BMI, body mass index; BP, blood pressure; OSA, obstructive sleep apnea.

show any significant differences in serum ICAM-1, VCAM-1, P-selectin, L-selectin, and E-selectin concentrations (Table 2) compared to the control subjects.

Comparison of Regional WM Integrity Loss between Groups

The location and extent of regions with significant differences in the FA map between the severe OSA and control groups are presented in Table 3. Patients with severe OSA had reduced FA values in the right medial temporal WM (parahippocampal gyrus), left superior longitudinal fasciculus (BA 39, BA2), bilateral parietal WM (BA 40, BA 7, right insula), right corticospinal tract, left inferior longitudinal fasciculus (BA 7), left cingulum (BA 24), right tapetum, left posterior corona radiata (BA 13), left external capsule, and right inferior fronto-occipital fasciculus (Figure 2).

In ROI analysis, nearly all brain regions in the OSA group had significantly reduced FA values compared to the control subjects, consistent with findings of whole-brain voxel-based analysis, except for regions in the left inferior longitudinal fasciculus, left cingulum, and left posterior corona radiate. Together with decreased FA values, WMs with increased RD were found in the left superior longitudinal fasciculus (BA 39), right parietal WM (insula), and right tapetum. No region exhibited significant group differences in MD and AD values.

Relationship between DTI Indices and Clinical Severity

Correlation analysis was used to evaluate the influence of clinical severity and DTI indices (Table 4). Scores of clinical severity included AHI, desaturation index, snoring index, and average O_2 saturation.

Relation between FA Value and Clinical Severity

In general, poorer PSG parameters were associated with poorer DTI indices. The AHI was negatively correlated with FA in the right medial temporal WM, bilateral parietal WM, left superior longitudinal fasciculus, right corticospinal tract, right

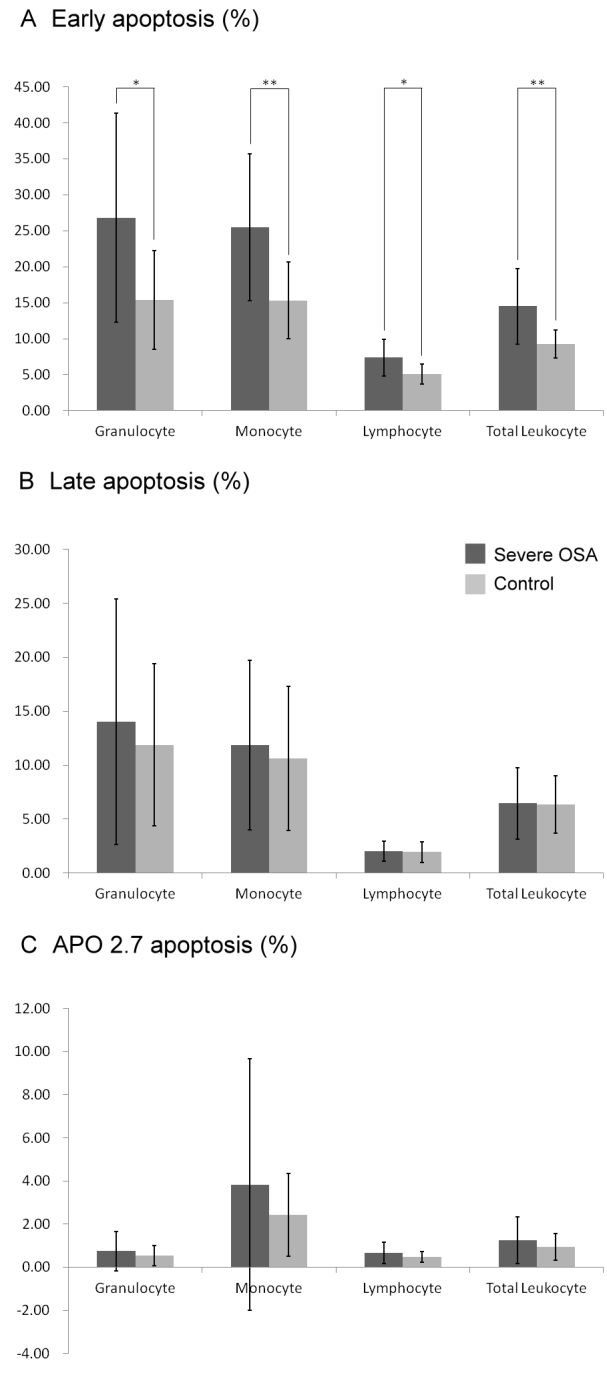

Figure 1—The percentages of **(A)** early apoptosis, **(B)** late apoptosis, and **(C)** APO 2.7 apoptosis in patients with severe obstructive sleep apnea (OSA) compared to control subjects. Apoptotic cells were defined as those that were APO 2.7 positive. Leukocyte subtypes were identified according to their CD45 expression intensity. The presence of late apoptotic cells meant that the cell membrane integrity was disrupted. The presence of early apoptotic cells indicated that the apoptotic change was early and still reversible. Early apoptosis of total leukocytes and their subsets, including granulocytes, monocytes, and lymphocytes, were significantly higher in the patients with OSA than in the controls. Data were the mean ± standard deviation. * P < 0.05 compared to controls. ** P < 0.01 compared to controls.

Table 2—Laboratory data of patients with severe obstructive sleep apnea and control subjects.

	Severe OSA (n = 20)	Control (n = 14)	P	F
$CD133^+/CD34^+$ (%)	21.144 ± 14.006	24.255 ± 12.025	0.451	0.507
$KDR^+/CD34^+$ (%)	1.204 ± 0.805	1.208 ± 0.947	0.676	0.418
ICAM-1	206.928 ± 81.034	176.667 ± 35.244	0.143	0.708
VCAM-1	533.260 ± 128.900	505.400 ± 108.771	0.689	0.414
P-selectin	81.743 ± 17.950	73.104 ± 20.904	1.184	0.286
L-selectin	1085.230 ± 164.608	1078.950 ± 178.381	0.084	0.774
E-selectin	44.279 ± 27.515	29.997 ± 15.433	0.456	0.505

Data are presented as mean ± standard deviation and compared by analysis of covariance after controlling for age, sex, body mass index, and systolic blood pressure. ICAM-1, intercellular adhesion molecule 1; KDR, kinase insert domain receptor; OSA, obstructive sleep apnea; VCAM-1, vascular cell adhesion molecule 1.

tapetum, and right inferior fronto-occipital fasciculus. The desaturation index was negatively correlated with FA in the right medial temporal WM, right parietal WM, right corticospinal tract, right tapetum, and right inferior fronto-occipital fasciculus. The snoring index revealed no statistically significant correlation with FA, whereas the average O_2 saturation was positively correlated with FA in the right medial temporal WM and right corticospinal tract. All the aforementioned statistically significant differences were maintained after correction to $P < 0.05$ for multiple comparisons.

Table 3—Regions showing fractional anisotropy differences among patients with severe obstructive sleep apnea and control subjects.

MNI Atlas Coordinates			Voxel		Brodmann		FA, mean (SD)			Diffusivity Values (OSA-NC) ($x10^{-6}$)		
X	Y	Z	Size	White Matter Tract	Area	Near Cortical Area	Controls	Severe OSA	t_{max}	MD	AD	RD
Decreased FA in Severe OSA Versus Controls												
31	−5	−34	455	Right medial temporal WM	–	R Parahippocampal Gyrus	0.275 (0.017)	0.238 (0.027)*	4.43	19	−16	36
−40	−51	33	608	Left superior longitudinal fasciculus	BA 39	L Pariental Lobe/Supramarginal Gyrus	0.421 (0.038)	0.361 (0.040)*	4.21	23	−45	57*
−52	−26	33	100	Left parietal WM	BA 40	L Inferior Parietal Lobule	0.293 (0.077)	0.207 (0.054)*	3.71	45	−38	86
17	−50	49	362	Right parietal WM	BA 7	L Precunenus	0.474 (0.033)	0.415 (0.036)*	3.67	7	−57	38
−35	−27	34	936	Left superior longitudinal fasciculus	BA 2	L Postcentral Gyrus	0.437 (0.021)	0.399 (0.025)*	3.66	31	1	46
8	−21	−21	712	Right corticospinal tract	–	R Cerebral Peduncle	0.546 (0.029)	0.503 (0.023)*	3.63	83	46	102
35	−15	16	918	Right parietal WM	–	R Insula/Claustrum	0.410 (0.027)	0.372 (0.016)*	3.54	7	−28	24*
−19	−68	34	108	Left inferior longitudinal fasciculus	BA 7	L Precunenus	0.452 (0.061)	0.381 (0.049)	3.50	2	−83	44
−6	29	20	128	Left cingulum	BA 24	L Anterior Cingulate	0.461 (0.042)	0.409 (0.083)	3.46	18	−42	48
33	−48	12	680	Right tapetum	–	R Tapetum	0.554 (0.022)	0.519 (0.024)*	3.40	31	−2	47*
−27	−27	19	244	Left posterior corona radiata	BA 13	L Insula	0.663 (0.026)	0.629 (0.029)	3.31	11	−30	32
−24	20	0	105	Left external capsule	–	L Putamen	0.451 (0.023)	0.416 (0.026)*	3.21	19	−14	35
38	−32	−2	239	Right inferior fronto-occipital fasciculus	–	R Caudate tail	0.508 (0.024)	0.479 (0.025)*	3.17	5	−35	25

Location of maximum effect (uncorrected $P < 0.005$, cluster size > 100) was shown in the Montreal Neurological Institute (MNI) space. Group FA mean values in each cluster are presented as mean (standard deviation). The FA, MD, AD, and RD values in region of interest were further compared between two groups by analysis of covariance after controlling for age, sex, body mass index, and systolic blood pressure. * $P < 0.05$ with a Bonferroni corrected, accounting for multiple ROI comparisons. AD, axial diffusivity; FA, fractional anisotropy; MD, mean diffusivity; NC, normal control; OSA, obstructive sleep apnea; RD, radial diffusivity; WM, white matter.

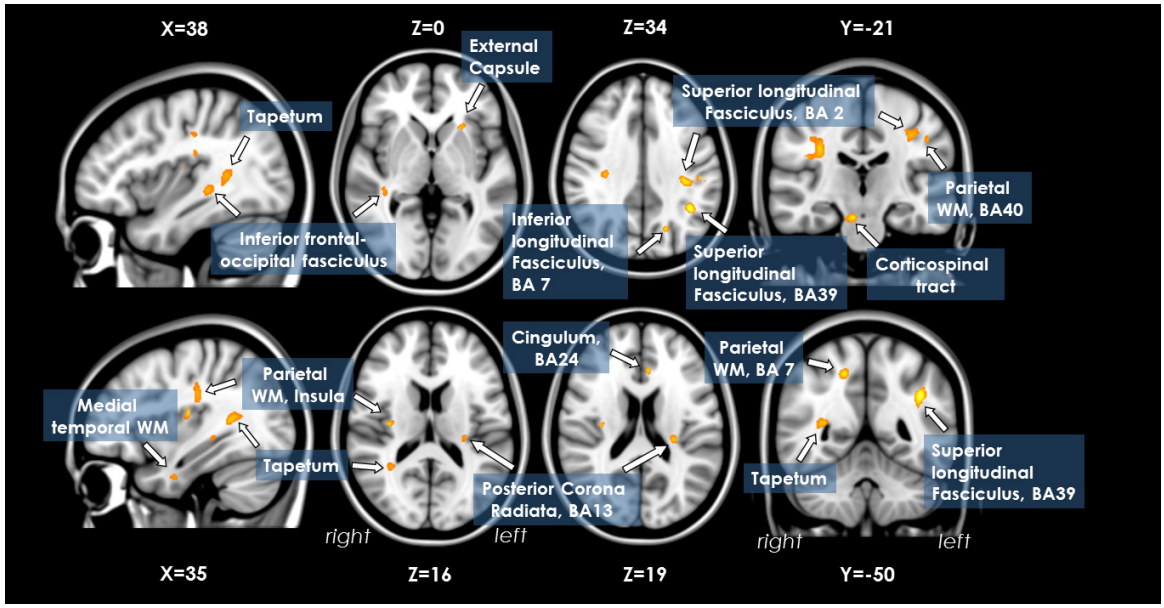

Figure 2—Lower fractional anisotropy values in patients with obstructive sleep apnea (n = 20) versus control subjects (n = 14) in the right medial temporal WM (parahippocampal gyrus), left superior longitudinal fasciculus (BA 39, BA2), bilateral parietal WM (BA 40, BA 7, right insula), right corticospinal tract, left inferior longitudinal fasciculus (BA 7), left cingulum (BA 24), right tapetum, left posterior corona radiata (BA 13), left external capsule, and right inferior fronto-occipital fasciculus. WM, white matter.

Table 4—Correlation among diffusion tensor abnormalities, clinical disease severity, and percentage of leukocyte early apoptosis.

	Correlation (r) of Clinical Variable							
Wm Tract	AHI	Desaturation Index	Average O_2 Saturation	Snoring Index	Granulocyte Early Apoptosis	Monocyte Early Apoptosis	Lymphocyte Early Apoptosis	WBC Early Apoptosis
FA								
Right medial temporal WM	−0.643 [b]	−0.649 [b]	0.576 [b]	−0.141	−0.417 [a]	−0.448 [a]	−0.338	−0.444 [a]
Left superior longitudinal fasciculus	−0.389 [a]	−0.351	0.123	−0.171	−0.280	−0.323	−0.280	−0.298
Left parietal WM	−0.536 [b]	−0.486 [a]	0.470 [a]	−0.051	−0.468 [a]	−0.379 [a]	−0.084	−0.325
Right parietal WM	−0.624 [b]	−0.557 [b]	0.422 [a]	−0.266	−0.214	−0.244	−0.314	−0.223
Left superior longitudinal fasciculus	−0.539 [b]	−0.481 [a]	0.326	−0.157	−0.397 [a]	−0.434 [a]	−0.393 [a]	−0.350
Right corticospinal tract	−0.782 [b]	−0.740 [b]	0.511 [b]	−0.379 [a]	−0.345	−0.448 [a]	−0.405 [a]	−0.447 [a]
Right parietal WM	−0.767 [b]	−0.668 [b]	0.390 [a]	−0.083	−0.316	−0.378 [a]	−0.303	−0.329
Right tapetum	−0.575 [b]	−0.531 [b]	0.316	−0.157	−0.432 [a]	−0.454 [a]	−0.175	−0.399 [a]
Left external capsule	−0.425 [a]	−0.414 [a]	0.337	−0.251	−0.395 [a]	−0.310	−0.199	−0.385 [a]
Right inferior fronto-occipital fasciculus	−0.556 [b]	−0.526 [b]	0.283	−0.116	−0.337	−0.332	−0.375 [a]	−0.355
RD								
Left superior longitudinal fasciculus	0.443 [b]	0.382 [a]	−0.156	0.084	0.368 [a]	0.364 [a]	0.431 [b]	0.376 [a]
Right parietal WM	0.556 [b]	0.534 [b]	−0.315	0.070	0.391 [a]	0.424 [a]	0.255	0.372 [a]
Right tapetum	0.436 [b]	0.368 [a]	−0.230	0.102	0.382 [a]	0.335	0.235	0.332

Correlation among diffusion tensor abnormalities, clinical disease severity, and percentage of leukocyte early apoptosis were performed by partial correlation after controlling for age, sex, body mass index, and systolic blood pressure. [a]$P < 0.05$, uncorrected. [b]$P < 0.05$ with a Bonferroni corrected, accounting for multiple region of interest comparisons. AHI, apnea-hypopnea index; FA, fractional anisotropy; RD, radial diffusivity; WBC, white blood cell; WM, white matter.

Relation between RD Value and Clinical Severity

The RD values in the left superior longitudinal fasciculus (BA39), right parietal WM (insula), and right tapetum were positively correlated with the AHI. The RD value in the right parietal WM (insula) was positively correlated with the desaturation index. All the aforementioned statistically significant differences were maintained after correction to $P < 0.05$ for multiple comparisons

Relationship between DTI Indices and Leukocyte Apoptosis

Results of the analysis regarding differences in the percentages of leukocyte early apoptosis and DTI indices are listed in Table 4 with corrected and uncorrected P values.

Relation between FA Value and Leukocyte Early Apoptosis

The percentages of early apoptosis of total leukocytes were negatively correlated with the FA values in the right medial temporal WM, right corticospinal tract, right tapetum, and left external capsule. In the analysis of leukocyte subsets, the percentages of early apoptosis of granulocytes were negatively correlated with the FA values in the right medial temporal WM, left parietal WM (BA 40), left superior longitudinal fasciculus (BA 2), right tapetum, and left external capsule. The percentages of early apoptosis of monocytes were negatively correlated with the FA values in the right medial temporal WM, left parietal WM (BA 40), left superior longitudinal fasciculus (BA 2), right corticospinal tract, right parietal WM (insula), and right tapetum. The percentages of early apoptosis of lymphocytes were negatively correlated with the FA values in the left superior longitudinal fasciculus (BA 2), right corticospinal tract, and right inferior fronto-occipital fasciculus. All the aforementioned statistically significant differences were maintained with an uncorrected $P < 0.05$, but were not maintained with a corrected P value threshold.

Relation between RD Value and Leukocyte Early Apoptosis

The percentages of early apoptosis of lymphocytes were positively correlated with the RD values in the left superior longitudinal fasciculus (BA 39) with a corrected P value.

In uncorrected P value analysis, the percentages of early apoptosis of total leukocyte were positively correlated with the RD values in the left superior longitudinal fasciculus (BA 39) and right parietal WM (insula). In the analysis of leukocyte subsets, the percentages of early apoptosis of granulocytes were positively correlated with the RD values in the left superior longitudinal fasciculus (BA 39), right parietal WM (insula), and right tapetum. The percentages of early apoptosis of monocytes were positively correlated with the RD values in the left superior longitudinal fasciculus (BA 39) and right parietal WM (insula).

DISCUSSION

In the comparison between patients with severe OSA and healthy controls, the patients with OSA presented with significantly increased AHI score, desaturation index, and snoring index, and decreased average O_2 saturation during sleep. In the evaluation of leukocyte apoptosis, the patients with OSA also showed significantly increased early apoptosis in total leukocytes and its subsets. Diffusion imaging revealed impaired fiber integrity in the patients with OSA, indicating increased WM microstructural damage. The WM damage was further associated with disease severity, as indicated by increased AHI and desaturation index, and decreased O_2 saturation. It was also associated with higher systemic inflammation as indicated by the marker of leukocyte early apoptosis. This study is the first to report an association between intracranial WM integrity and circulating inflammatory markers in patients with OSA.

Patients with OSA experience repetitive episodes of hypoxia/reoxygenation during transient cessation of breathing

that promote systemic oxidative stress and inflammation.[22] Normal endothelium regulates vasomotor tone and preserves inflammatory and coagulation hemostasis,[23] but these functions are altered in patients with OSA. Repetitive hypoxia/reoxygenation is considered the main culprit for impaired endothelial function.[24] Enhanced release of superoxide by polymorphonuclear leukocytes derived from patients with OSA points to enhanced systemic oxidative stress in OSA.[25] The results of the current study are consistent with those of previous investigations but provide a much more detailed examination of leukocyte apoptosis.

The results here reveal increased leukocyte early apoptosis, mostly in monocytes, in the OSA group. That the early apoptotic leukocytes detected via flow cytometry through phosphatidylserine expression were positive only for the annexin V marker but negative for 7-AAD means that changes occur at the cell surface. During the initial stages of apoptosis, the cell membrane remains intact. At the very moment that necrosis occurs, the cell membrane loses its integrity and becomes leaky.

In related research,[26] the monocyte expression of the adhesion molecules CD15 and CD11c was found to be increased in patients with OSA compared to controls. Patients with OSA also have increased intracellular reactive oxygen species production in some monocyte and granulocyte subpopulations. It is known that repetitive hypoxia/reoxygenation promotes endothelial apoptosis by activating cell death receptors and mitochondria-dependent apoptotic pathways.[27] However, little attention has been given to leukocyte apoptosis. In the current study, the significant leukocyte apoptosis mainly in early apoptosis suggests that the damage has not been carried to irreversible change.[28]

Newly diagnosed, untreated patients with OSA show significantly reduced global brain FA values, and these changes have been localized in various brain regions in the current study. The nature of lower FA changes in OSA reflects alterations in WM fiber integrity. Decreased FA primarily represents axonal groups that are damaged, shrunken, or have less myelin.[29] This decrease occurs after either an increase in RD or a decrease in AD, or both. Increased RD reflects increased water diffusion in the perpendicular direction. Decreased FA with increased RD in the left superior longitudinal fasciculus (BA 39), right parietal WM (insula), and right tapetum have been suggested as being predominantly caused by myelin disruption or loss.[30] However, decreased FA with reduced AD but increased RD may likewise be associated with axonal damage and demyelination or the fiber reorganization found in neurotoxic diseases.[31]

In the current study, another pattern of DTI index changes revealed decreased FA without significant changes in AD, RD, and MD, such as in the right medial temporal WM, left parietal WM (BA 40), right parietal WM (BA 7), left superior longitudinal fasciculus (BA 2), right corticospinal tract, left external capsule, and right inferior fronto-occipital fasciculus. It is generally agreed that alternations of fiber tract integrity may occur in patients with OSA. However, multiple etiologies might contribute to similar tensor appearance. Decreased FA has previously been reported in demyelination (such as in cases of multiple sclerosis[32]), axonal damage (such as in cases of trauma[33]), and gliosis (such as in cases of meningitis[34]). Thus, it might be difficult to clarify the pathophysiology in this cross-sectional study.

Our DTI results were consistent with most findings in previous OSA studies, including the findings that regional WM damage occurs in fibers of the anterior and posterior cingulate cortex and cingulum bundle; portions of the frontal, ventral prefrontal, parietal, and insular cortices; the bilateral internal capsule; the cerebral peduncle; and the corticospinal tract.[13] The WM regions with significant group differences in the current study were further found to be associated with increased disease severity. Using DTI, similar results regarding hypoxia insults have also been observed in conditions such as carbon dioxide intoxication and in adolescents born preterm, further corroborating the results here.[35,36] This study explores the possible etiology in OSA and posits that DTI is a good modality to assess the underlying pathophysiology of WM in OSA.

In a previous meta-analysis neuroimaging study,[37] significant gray matter reductions in patients with OSA occurred in the bilateral parahippocampus, whereas less convincing reductions occurred in the frontotemporal region, which may be related to neurocognitive processing abnormalities. Intermittent hypoxia and sleep fragmentation independently can lead to neuronal deficits in the hippocampus and prefrontal cortex.[38] Gao et al. reported that impaired corticospinal tract and external capsule with decreased FA and increased RD occurred in mild hypoxic-ischemic neonates,[39] leading to subsequent poor motor and cognitive performance. In Bregant et al.'s study,[40] a significant cortical volume reduction in the parahippocampal gyrus, the parietal lobe, and the temporal lobe was found in patients with hypoxic-ischemic encephalopathy. The current findings of fiber integrity alteration in patients with OSA may be considered as comprehensive results of hypoxic change. Similar results with anatomic deficits further underscore the vulnerability in this specific location.

The higher RD change of the left superior longitudinal fasciculus (BA39) is highly pertinent to increased lymphocyte early apoptosis. The lower FA change in most of the vulnerable brain regions is also related to increased leukocyte early apoptosis, even though these correlations were not maintained in rigorous statistical analysis. The relationship between alternations of WM integrity and systemic inflammation in terms of uncorrected P value can be considered meaningful because the statistical control was very strict in order to reduce possible variation.

To date, the current study is the first to demonstrate a correlation between WM fiber integrity change and a peripheral inflammatory marker. There are two kinds of pathophysiologic mechanisms possible to explain the study's findings: (1) systemic inflammatory change with cerebral involvement, or (2) primary cerebral inflammation with subsequent elevation of peripheral mediators. Increased levels of plasma C-reactive protein, leukocyte superoxide, and soluble adhesion molecules suggest the presence of chronic inflammation in patients with OSA.[24] Accumulation and adhesion of circulating leukocytes to the vascular endothelium leads to vessel inflammation and the progression of atherosclerosis.[41] Reduced nitric oxide availability results in endothelial dysfunction, which increases the risk for intracranial vessel diseases.[24] Vascular endothelial inflammation and enhanced oxidative stress may partly explain

the accelerated progression of intracranial atherosclerosis and the consequent WM damage in patients with untreated OSA.[13]

However, nonpreferential mobilization of white blood cells into the circulation was observed within 1 day after global hypoxia-ischemia, and a significant influx of neutrophils into the brain was detected 7 days after the insult.[42] Such findings underscore that global hypoxia-ischemia may result in profound cerebral inflammation and mobilization of the peripheral innate immune system. Moreover, the expressions of monocyte chemotactic protein-1 and tumor necrosis factor (TNF)-α are reportedly increased in the brains of aged mice 7 days after WM stroke, correlating with a more distributed microglial activation.[43] In OSA, hypoxia results in the activation of inflammatory pathways such as those mediated by nuclear factor of kappa-B (NFκB), with downstream products of NFκB activation, including TNF-α, interleukin-6, interleukin-8, and ICAM-1 detected. The results here support the hypothesis that cytokine-mediated damage in the cardiovascular complications of OSA may partially contribute to alterations in WM integrity. Further understanding of the identity of the source cells that sense intermittent hypoxia and induce cytokine production with subsequent WM injury is imperative.

Although the current study has yielded useful findings, its design is not without flaws. The report fails to demonstrate any difference in circulating EPCs and soluble ICAM levels between the severe OSA and control groups, presumably because of the small sample size. Furthermore, it is important to emphasize that this is a cross-sectional study, which limits its interpretation of the whole view and complicated details of OSA. Future longitudinal studies of this cohort may help to verify the results and clarify the oxidative stress changes before and after treatment.

In conclusion, OSA can impair WM integrity in vulnerable regions, and this impairment is associated with increased disease severity. The possible interactions between systemic inflammation and central nervous system microstructural damage may represent variant hypoxic patterns and their consequent processes in OSA.

ACKNOWLEDGMENTS

The authors wish to thank the MRI Core Facility of CGMH, as well as Yi-Wen Chen, Ting-Yi Chen, and Yi-Fan Chiang, and all subjects who participated in this study. The authors also thank Drs. Meng-Chih Lin, Mao-Chang Su, Chien-Hung Chin, and Yung-Che Chen for their assistance in the sleep studies and manuscript preparation.

DISCLOSURE STATEMENT

This was not an industry supported study. This work was supported by grants from the National Science Council of the Republic of China (NSC NMRPG 8B6142 to H-L Chen and Chang Gung Medical Research Project CMRPG 8C0021 to P-C Chen). The authors have indicated no financial conflicts of interest.

REFERENCES

1. Marin JM, Carrizo SJ, Vicente E, Agusti AG. Long-term cardiovascular outcomes in men with obstructive sleep apnoea-hypopnoea with or without treatment with continuous positive airway pressure: an observational study. Lancet 2005;365:1046–53.
2. Yaggi HK, Concato J, Kernan WN, Lichtman JH, Brass LM, Mohsenin V. Obstructive sleep apnea as a risk factor for stroke and death. N Engl J Med 2005;353:2034–41.
3. Lavie L, Polotsky V. Cardiovascular aspects in obstructive sleep apnea syndrome - molecular issues, hypoxia and cytokine profiles. Respiration 2009;78:361–70.
4. Lavie L, Dyugovskaya L, Polyakov A. Biology of peripheral blood cells in obstructive sleep apnea--the tip of the iceberg. Arch Physiol Biochem 2008;114:244–54.
5. Werner N, Kosiol S, Schiegl T, et al. Circulating endothelial progenitor cells and cardiovascular outcomes. N Engl J Med 2005;353:999–1007.
6. Carson MJ, Thrash JC, Walter B. The cellular response in neuroinflammation: the role of leukocytes, microglia and astrocytes in neuronal death and survival. Clin Neurosci Res 2006;6:237–45.
7. Lee SJ, Benveniste EN. Adhesion molecule expression and regulation on cells of the central nervous system. J Neuroimmunol 1999;98:77–88.
8. Langer HF, Chavakis T. Leukocyte-endothelial interactions in inflammation. J Cell Mol Med 2009;13:1211–20.
9. Gilgun-Sherki Y, Melamed E, Offen D. The role of oxidative stress in the pathogenesis of multiple sclerosis: the need for effective antioxidant therapy. J Neurol 2004;251:261–8.
10. Kokturk O, Ciftci TU, Mollarecep E, Ciftci B. Elevated C-reactive protein levels and increased cardiovascular risk in patients with obstructive sleep apnea syndrome. Int Heart J 2005;46:801–9.
11. Xu W, Chi L, Row BW, et al. Increased oxidative stress is associated with chronic intermittent hypoxia-mediated brain cortical neuronal cell apoptosis in a mouse model of sleep apnea. Neuroscience 2004;126:313–23.
12. Kumar R, Chavez AS, Macey PM, Woo MA, Yan-Go FL, Harper RM. Altered global and regional brain mean diffusivity in patients with obstructive sleep apnea. J Neurosci Res 2012;90:2043–52.
13. Macey PM, Kumar R, Woo MA, Valladares EM, Yan-Go FL, Harper RM. Brain structural changes in obstructive sleep apnea. Sleep 2008;31:967–77.
14. Sleep-related breathing disorders in adults: recommendations for syndrome definition and measurement techniques in clinical research. The report of an American Academy of Sleep Medicine Task Force. Sleep 1999;22:667–89.
15. Tan TY, Liou CW, Friedman M, Lin HC, Chang HW, Lin MC. Factors associated with increased carotid intima-media thickness in obstructive sleep apnea/hypopnea syndrome. Neurologist 2012;18:277–81.
16. Kushida CA, Littner MR, Morgenthaler T, et al. Practice parameters for the indications for polysomnography and related procedures: an update for 2005. Sleep 2005;28:499–521.
17. Kales A, Rechtschaffen A; University of California LABISNNINUS. A manual of standardized terminology, techniques and scoring system for sleep stages of human subjects. Bethesda, MD: U S National Institute of Neurological Diseases and Blindness, Neurological Information Network, 1968.
18. Koester SK, Roth P, Mikulka WR, Schlossman SF, Zhang C, Bolton WE. Monitoring early cellular responses in apoptosis is aided by the mitochondrial membrane protein-specific monoclonal antibody APO2.7. Cytometry 1997;29:306–12.
19. Yip HK, Chang LT, Chang WN, et al. Level and value of circulating endothelial progenitor cells in patients after acute ischemic stroke. Stroke 2008;39:69–74.
20. Wang HC, Lin WC, Lin YJ, et al. The association between serum adhesion molecules and outcome in acute spontaneous intracerebral hemorrhage. Crit Care 2011;15:R284.
21. Jenkinson M, Beckmann CF, Behrens TEJ, Woolrich MW, Smith SM. FSL. NeuroImage 2012;62:782–90.
22. Jelic S, Le Jemtel TH. Inflammation, oxidative stress, and the vascular endothelium in obstructive sleep apnea. Trends Cardiovasc Med 2008;18:253–60.
23. Aird WC. Phenotypic heterogeneity of the endothelium: II. Representative vascular beds. Circ Res 2007;100:174–90.
24. Atkeson A, Jelic S. Mechanisms of endothelial dysfunction in obstructive sleep apnea. Vasc Health Risk Manag 2008;4:1327–35.
25. Schulz R, Mahmoudi S, Hattar K, et al. Enhanced release of superoxide from polymorphonuclear neutrophils in obstructive sleep apnea. Impact of continuous positive airway pressure therapy. Am J Respir Crit Care Med 2000;162:566–70.

26. Dyugovskaya L, Lavie P, Lavie L. Increased adhesion molecules expression and production of reactive oxygen species in leukocytes of sleep apnea patients. Am J Respir Crit Care Med 2002;165:934–9.
27. Dhar-Mascareno M, Carcamo JM, Golde DW. Hypoxia-reoxygenation-induced mitochondrial damage and apoptosis in human endothelial cells are inhibited by vitamin C. Free Rad Biol Med 2005;38:1311–22.
28. Kabara E, Coussens PM. Infection of primary bovine macrophages with Mycobacterium avium subspecies paratuberculosis suppresses host cell apoptosis. Front Microbiol 2012;3:215.
29. Madden DJ, Bennett IJ, Burzynska A, Potter GG, Chen NK, Song AW. Diffusion tensor imaging of cerebral white matter integrity in cognitive aging. Biochim Biophys Acta 2012;1822:386–400.
30. Song SK, Yoshino J, Le TQ, et al. Demyelination increases radial diffusivity in corpus callosum of mouse brain. NeuroImage 2005;26:132–40.
31. Lin WC, Chou KH, Chen CC, et al. White matter abnormalities correlating with memory and depression in heroin users under methadone maintenance treatment. PLoS One 2012;7:e33809.
32. Sbardella E, Petsas N, Tona F, et al. Assessing the correlation between grey and white matter damage with motor and cognitive impairment in multiple sclerosis patients. PLoS One 2013;8:e63250.
33. Jang SH. Diffusion tensor imaging studies on corticospinal tract injury following traumatic brain injury: a review. NeuroRehabilitation 2011;29:339–45.
34. Lu CH, Chen HL, Chang WN, et al. Assessing the chronic neuropsychologic sequelae of human immunodeficiency virus-negative cryptococcal meningitis by using diffusion tensor imaging. AJNR Am J Neuroradiol 2011;32:1333–9.
35. Lin WC, Lu CH, Lee YC, et al. White matter damage in carbon monoxide intoxication assessed in vivo using diffusion tensor MR imaging. AJNR Am J Neuroradiol 2009;30:1248–55.
36. Groeschel S, Tournier JD, Northam GB, et al. Identification and interpretation of microstructural abnormalities in motor pathways in adolescents born preterm. NeuroImage 2014;87:209–19.
37. Weng HH, Tsai YH, Chen CF, Lin YC, Yang CT, Yang CY. Mapping gray matter reductions in obstructive sleep apnea: an activation likelihood estimation meta-analysis. Sleep 2014;37:167–75.
38. Row BW, Liu R, Xu W, Kheirandish L, Gozal D. Intermittent hypoxia is associated with oxidative stress and spatial learning deficits in the rat. Am J Respir Crit Care Med 2003;167:1548–53.
39. Gao J, Li X, Hou X, et al. Tract-based spatial statistics (TBSS): application to detecting white matter tract variation in mild hypoxic-ischemic neonates. Conf Proc IEEE Eng Med Biol Soc 2012;2012:432–5.
40. Bregant T, Rados M, Vasung L, et al. Region-specific reduction in brain volume in young adults with perinatal hypoxic-ischaemic encephalopathy. Eur J Paediatr Neurol 2013;17:608–14.
41. Price DT, Loscalzo J. Cellular adhesion molecules and atherogenesis. Am J Med 1999;107:85–97.
42. Jellema RK, Lima Passos V, Zwanenburg A, et al. Cerebral inflammation and mobilization of the peripheral immune system following global hypoxia-ischemia in preterm sheep. J Neuroinflammation 2013;10:13.
43. Rosenzweig S, Carmichael ST. Age-dependent exacerbation of white matter stroke outcomes: a role for oxidative damage and inflammatory mediators. Stroke 2013;44:2579–86.